


## Article

# Salivary pH Effect on Orthodontic Appliances: In Vitro Study of the SS/DLC System

António Fróis <sup>1,2</sup> , Manuel Evaristo <sup>1</sup>, Ana Cristina Santos <sup>1,2,3</sup> and Cristina Santos Louro <sup>1,\*</sup> 

<sup>1</sup> CEMMPRE, Department of Mechanical Engineering, University of Coimbra, 3030-788 Coimbra, Portugal; antonio.frois@student.uc.pt (A.F.); manuel.evaristo@dem.uc.pt (M.E.); acsantos@fmed.uc.pt (A.C.S.)

<sup>2</sup> Center for Innovative Biomedicine and Biotechnology (iCBR/CIBB), Biophysics Institute, Faculty of Medicine, University of Coimbra, 3000-548 Coimbra, Portugal

<sup>3</sup> Area of Environment Genetics and Oncobiology (CIMAGO), University of Coimbra, 3000-548 Coimbra, Portugal

\* Correspondence: cristina.louro@dem.uc.pt

**Abstract:** Stainless steels (SS) are the most-used alloys for manufacturing fixed orthodontic appliances due to their attractive set of mechanical properties, biocompatibility, and high corrosion resistance. Nevertheless, during regular orthodontic treatments—taking at least around 2 years—the intraoral environment inevitably degrades these bioalloys, releasing metallic ions into the oral cavity. In the first part of this in vitro study, the corrosion resistance of commercial SS appliances (brackets, tubes, and bands) was evaluated in Fusayama-Meyer artificial saliva at pH values of 2.3 and 6.8 over the course of 30 days. As expected, the results corroborated that salivary pH highly influences corrosion behaviour. Released Ni, Cr, and Fe were within dietary intake values. In the second part, a novel approach for oral corrosion prevention based on the chemical inertness of DLC materials is presented. SS surfaces were functionalized with biocompatible a-C:H-sputtered coatings and submitted to the same experimental conditions. The anticorrosion ability of this system was demonstrated, preventing the pitting corrosion that occurred on the SS substrates. Despite the galvanic coupling effect due to the presence of the Cr-based interlayer, this study enhanced the potential use of the reactive sputter-deposited a-C:H coatings in orthodontics.

**Keywords:** DLC coatings; stainless steel; corrosion; orthodontics



**Citation:** Fróis, A.; Evaristo, M.; Santos, A.C.; Louro, C.S. Salivary pH Effect on Orthodontic Appliances: In Vitro Study of the SS/DLC System. *Coatings* **2021**, *11*, 1302. <https://doi.org/10.3390/coatings11111302>

Academic Editor: Fabio Palumbo

Received: 28 September 2021

Accepted: 22 October 2021

Published: 27 October 2021

**Publisher's Note:** MDPI stays neutral with regard to jurisdictional claims in published maps and institutional affiliations.



**Copyright:** © 2021 by the authors. Licensee MDPI, Basel, Switzerland. This article is an open access article distributed under the terms and conditions of the Creative Commons Attribution (CC BY) license (<https://creativecommons.org/licenses/by/4.0/>).

## 1. Introduction

The European Union (EU) forbids the use of Nickel (Ni) [1]:

- (a) «in any post-assemblies which are inserted into pierced ears and other pierced parts of the human body unless the rate of nickel release from such post-assemblies is less than  $0.2 \mu\text{g}/\text{cm}^2/\text{week}$  (migration limit)»;
- (b) «in articles intended to come into direct and prolonged contact with the skin ( . . . ) if the rate of nickel release from the parts of these articles coming into direct and prolonged contact with the skin is greater than  $0.5 \mu\text{g}/\text{cm}^2/\text{week}$ »;
- (c) «in articles referred to in point (b) where these have a non-nickel coating unless such coating is sufficient to ensure that the rate of nickel release from those parts of such articles coming into direct and prolonged contact with the skin will not exceed  $0.5 \mu\text{g}/\text{cm}^2/\text{week}$  for a period of at least two years of normal use of the article».

However, metallic biomedical alloys lie outside this EU regulation regarding this matter.

In contemporary orthodontics, malocclusions are usually treated with fixed orthodontic appliances, which are systems composed of brackets, archwires, tubes and/or bands tightened by ligatures and bonded to the teeth with adhesives or resins [2,3]. Since a regular orthodontic treatment takes at least around 2 years [4], the biocompatibility of the materials employed is of utmost importance.

Biometallic alloys, such as Nitinol (NiTi) and stainless steels (SS), are preferred over other classes of materials to manufacture fixed orthodontic appliances due to their wide range of properties, including superior *in vivo* mechanical behaviour [3]. However, the oral cavity is a dynamic and complex system where metallic ion release inevitably occurs due to multiple changing variables: chemical composition, temperature and pH, different diets, oral flora and its byproducts, oral hygiene, and health and psychosomatic conditions of each individual [5–11]. Corrosion with metallic species release is the end result. Important consequences of this deleterious oral reaction include discoloration of the enamel, hypersensitivity, inflammatory reactions, and toxicity effects [5,7,12,13].

Some released metallic species are toxic and/or can induce allergic reactions [5,7,14]. Among them, Ni stands out: (i) The International Agency for Research on Cancer (IARC) classifies Ni<sup>2+</sup> and all its compounds as carcinogenic or potentially carcinogenic to humans [12]; (ii) Ni is a strong immunologic sensitizer, capable of triggering cytotoxic and mutagenic effects [14,15]; (iii) Ni<sup>2+</sup> can affect cellular functions, inducing apoptosis and modifying gene expression [14,15].

Reported intra- to extraoral and subtle to severe symptoms of allergy to Ni-containing orthodontic components include a burning sensation, generalized urticaria, and widespread eczema [7,16–18]. While, in general, the impact of Ni-related allergies in orthodontics seems low and non-consensual [5–7], Ni allergies may easily be underdiagnosed [6,18].

Despite concerns, Ni-containing alloys are still used, since metal-free alternative solutions still face multiple concerns that undermine clinicians' acceptance [2,3,19]. Surface engineering provides two options to enhance the properties of metallic surfaces: surface modification or coating deposition [20]. Aspiring to a safe future, the second alternative was chosen in this study.

Amorphous carbon films, also termed diamond-like carbon (DLC) films [21], are extensively used and/or studied as protective coatings for several industrial applications [22], including to prevent tribocorrosion of metallic parts [23]. These coatings are clearly attractive for biomedical applications due to their excellent biocompatibility [24]. The hydrogenated forms of amorphous carbon, a-C:H, constitute a major group of DLC materials with H contents up to 60 at.% [25]. Together with H content, the sp<sup>2</sup>/sp<sup>3</sup> C–C bond ratio rules the final properties of DLCs [21], which can be further tuned by doping [23]. One of the major disadvantages of DLC coatings is the low long-term adhesion to substrates [26], which can be improved by depositing a metallic-based interlayer between the substrate and the C-based coating [23,27]. To the authors' knowledge, little research has been carried out in orthodontics when compared to other medical fields (e.g., orthopaedics [26,27]), despite encouraging results already published [28–30].

In a previous research work, the authors discussed the reactive CH<sub>4</sub> flow effect on the microstructure, hardness, and biological behavior of sputtered, deposited a-C:H coatings. The cell viability of the a-C:H/AISI 316L system was confirmed using two types of cells: macrophages and fibroblasts, either in mono or coculture with extracts, for estimated H contents in the range of 28–40 at.%. The highest biocompatibility was found for coatings with the lowest H content [31]. Following this important result, the present study addresses the synthesis of the a-C:H coatings with lower H content, by sputtering, on SS substrates with higher Ni nominal content (AISI 310). The goal for the work persists: to functionalize the surface against metallic diffusion into the oral cavity without compromising biocompatibility and the SS bulk properties.

In the first part of this *in vitro* study, the corrosion behaviour of commercially available brackets, tubes, and bands was assessed in Fusayama-Meyer artificial saliva for 30 days. Two pH values were selected: one close to the oral physiological value (pH = 6.8) and the other according to ISO 10271:2001 (pH = 2.3) [32]. The second part regards a-C:H films deposited by reactive magnetron sputtering—a clean, highly versatile, and low-cost technology—to improve surface properties of SS alloys. The previously cited experimental conditions were also used to simulate the oral conditions *in vitro* [31].

## 2. Materials and Methods

### 2.1. Materials

#### 2.1.1. Orthodontic Components

Typical commercially available Ni-containing components of orthodontic appliances were used in this study (Figure 1), whose characteristics are summarized in Table 1. Table 1 also includes the nominal composition of the AISI 310 substrates used for coating deposition, which were selected due to their exceptionally higher Ni content (>20 wt.%) in comparison to conventional orthodontic SS grades.

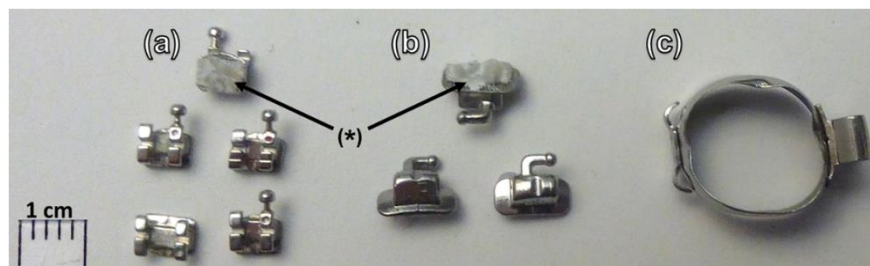


**Figure 1.** Representative orthodontic components used in this study: (a) brackets, (b) tubes, and (c) band (with attached tube). The resin-covered bases of a bracket and a tube are highlighted (\*).

**Table 1.** Nominal chemical composition of the commercially available SS components of fixed orthodontic appliances and AISI310 substrates.

Component	Grade	Composition (wt.%)						
		Ni	Cr	C	Mn	Si	Cu	Fe
Brackets <sup>1</sup>	AISI303	8–10	17–19	≤0.15	≤2	≤1	-	Balance
Tubes <sup>2</sup>	AISI630	3–5	15–18	≤0.07	≤2	≤1	3–5	Balance
Bands <sup>1</sup>	AISI305	11–13	17–19	≤0.12	≤2	≤1	-	Balance
Substrates for coatings	AISI310	19–22	24–26	≤0.25	≤2	≤1.5	-	Balance

Suppliers: <sup>1</sup> Ormco™, Orange, CA, USA; <sup>2</sup> Morelli™, Sorocaba, SP, Brazil.

#### 2.1.2. a-C:H Coatings

Hydrogenated amorphous carbon coatings, a-C:H, were synthesized by reactive magnetron sputtering (Teer Coating equipment, TEER Coating Ltd., Worcestershire, UK) in the direct-current (dc) discharge regime, with two C and one Cr target (purity > 99.9%). The SS316L surface preparation followed the “traditional” approach for coating deposition: samples were grinded with SiC sandpaper (P500 to P2000) and mirror-polished with 3 μm diamond suspension. All samples were ultrasonically cleaned in an acetone/alcohol bath and dried by hot airflow. Preceding the external a-C:H layer deposition, substrates were sputter-etched with Ar+ bombardment for 30 min to remove surface impurities, followed by a Cr-based buffer layer formation of ~300 nm (Cr and C targets power of 2000 and 50 W, respectively) to improve adhesion of the coatings to the metallic substrates. The deposition parameters were maintained constantly: total working gas pressure of 0.6 Pa, Ar flow of 46 sccm, CH<sub>4</sub> flow of 5 sccm, negative substrate bias of −50 V, 2 graphite targets (99.9% purity) with a constant power of 1750 W. The deposition time was selected to achieve a total coating thickness close to 1 μm [31,33]. To facilitate reading, coated and uncoated AISI310 samples will be termed as a-C:5H and SS310, respectively.

### 2.2. Corrosion Tests

Corrosion tests were performed in an immersion solution of Fusayama-Meyer artificial saliva (Table 2), following ISO 10271: *Dental metallic materials—Corrosion Test methods* [32] and other research works [31,33,34]. For the SS310 samples and a-C:5H coatings, a ratio of 1 cm<sup>2</sup> of sample surface area per 10 mL of solution was used, while for the fixed orthodontic

components (10 brackets, 2 bands and 6 tubes), a ratio of 0.02 mg per 1 mL of saliva was chosen. Two pH solution values were selected: 6.8 and 2.3. Before the tests, the base of the brackets and tubes were covered with commonly used orthodontic resin (Transbond™, 3M™, St. Paul, MN, USA) (see Figure 1) to inhibit corrosion from those surfaces, similar to the real oral use. After immersion, samples were ultrasonically cleaned in alcohol and air dried prior to characterization.

**Table 2.** Chemical composition of the Fusayama-Meyer artificial saliva.

Concentration [g/L]						
NaCl	KCl	CaCl <sub>2</sub> ·2H <sub>2</sub> O	NaH <sub>2</sub> PO <sub>4</sub>	Na <sub>2</sub> S·9H <sub>2</sub> O	CO (NH <sub>2</sub> ) <sub>2</sub>	HCl (1M)
0.4	0.4	0.795	0.78	0.005	1	until pH 6.8 or 2.3

### 2.3. Characterization Procedure

Quantitative analysis of Ni, Cr, and Fe released into the artificial saliva was performed in duplicate by inductively coupled plasma-optical emission spectroscopy (ICP-OES) in a PerkinElmer-Optima 8000 series spectrometer (PerkinElmer, Inc., Waltham, MA, USA). All solutions were previously acidified by adding 1 mL of HNO<sub>3</sub> (65%) per 5 mL of saliva and diluted twice to reach a final volume of 10 mL. The ICP detection limits were 5 µg/L for Ni and 10 µg/L for Cr and Fe. The average metal-release rates (µg per day and per g) were estimated. SS310 samples were used as reference for the a-C:5H coatings.

The surface and cross-section morphologies were observed by high-resolution scanning electron microscopy (SEM-ZEISS Merlin Compact/VP Compact, Oberkochen, Germany). Both chemical composition and elemental distribution maps were obtained through energy-dispersive spectroscopy (EDS-coupled Oxford X-Max Instruments to the SEM system, Oxford Instruments, Oxford, UK).

Structural and chemical bonding were studied through visible Raman spectroscopy (LabRAM HR Evolution, Horiba, 532 nm wavelength, Kyoto, Japan). Raman spectra were deconvoluted in the D and G bands by using a Gaussian-type fitting [21,35]. An additional band at ~1250 cm<sup>-1</sup> was considered to obtain proper fittings [35–37]. The C–C sp<sup>3</sup> hybridization fraction was calculated using Equation (1),

$$\% sp^3 = [0.24 - 48.9 (w_G - 0.1580)] \times 100, \quad (1)$$

where  $w_G$  is the position of the G peak in the inverse of micrometer unit (µm<sup>-1</sup>) [38].

Phase composition of the coatings was characterized by Fourier-transform infrared spectroscopy (FTIR) in the attenuated total reflection (ATR) mode (Smart Orbit, Nicolet 380, Thermo Fisher Scientific, Waltham, MA, USA). Normalized absorbance spectra of coatings are presented, summarizing at least 3 measurements per sample. The FTIR spectra were deconvoluted in 9 Gaussian-type bands corresponding to the known vibrational frequencies of a-C:H in the infrared absorption range of 2800–3100 cm<sup>-1</sup> [21]. Note that a possible band at 3300 cm<sup>-1</sup>, for C-H bonds with the sp<sup>1</sup> carbon configuration [21], was absent; therefore, spectra were analysed at around 3100 cm<sup>-1</sup> and include all sp<sup>2</sup>- and sp<sup>3</sup>-C hybridization assignments of C-H bonds. The sp<sup>3</sup>/sp<sup>2</sup> ratio was estimated by applying Equation (2) to all peak areas,

$$\frac{sp^3}{sp^2} = \frac{A_5 + A_6 + A_7 + A_8 + A_9}{A_1 + A_2 + A_3 + A_4}. \quad (2)$$

The average surface roughness (Ra) was measured by atomic force microscopy (AFM-Veeco DiInnova, Barcelona, Spain) running in intermittent mode (vibration frequency of 11 to 19 kHz) on a 2 × 2 µm<sup>2</sup> area. An OCA contact angle measuring system (DataPhysics Instruments GmbH, Filderstadt, Germany) was used to assess the static contact angles, applying distilled water (at least three measurements per sample).

Mechanical properties were evaluated by depth-sensing indentation (DSI), using a Berkovich indenter (MicroMaterials NanoTest platform, Wrexham, UK). Nanohardness

values were obtained from an average of 20 indentations performed under a nominal load of 5 mN, with a maximum indentation depth below 10% of the coatings' thickness. The H content of the a-C:5H coatings was estimated from their nanohardness knowledge by using Equation (3) [38],

$$\text{Hardness [GPa]} = 44.195 - 0.93 \times H_{\text{content}}[\text{at.\%}]. \quad (3)$$

### 3. Results and Discussion

#### 3.1. Orthodontic Components

The ICP results of orthodontic SS components are summarized in Table 3, and Figure 2 shows the metal release rates, as a function of the artificial saliva pH. Three main conclusions arise from the analysis of these corrosion data:

1. The increased rate of metallic element release is evident in the decreasing pH of the saliva;
2. Ni is released in a higher rate than Cr for all orthodontic components;
3. Ni release during the sampling period is significantly higher for brackets in comparison to tubes and bands at pH = 2.3.

**Table 3.** ICP-OES data concerning Ni, Cr, and Fe release.

Samples	Days	pH	Concentration ( $\mu\text{g/L}$ )		
			Ni	Cr	Fe
Brackets	30	6.8	54	24	218
		2.3	75,020	24,380	138,960
Tubes	30	6.8	11	<LD	90
		2.3	691	2162	10,723
Bands	30	6.8	363	125	2710
		2.3	593	812	4608
SS310	7	6.8	17	<LD	145
		2.3	38	29	256
	30	6.8	20	23	182
		2.3	42	35	356
a-C:H	7	6.8	12	<LD	69
		2.3	34	40	217
	30	6.8	12	21	77
		2.3	64	51	345

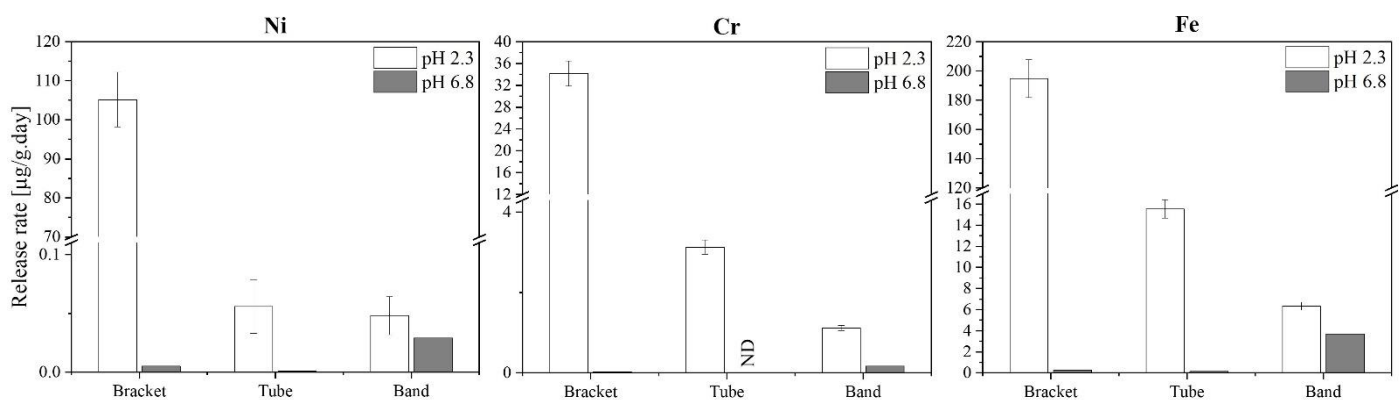


**Figure 2.** Average release rates of Ni, Cr, and Fe of fixed orthodontic components. ND: not detected.

The AISI303 brackets presented a lower in vitro corrosion resistance, corroborated by the highest release rates of all elements in the acidic saliva (pH = 2.3), Figure 2. Fe was, undoubtedly, the main released element ( $\sim 195 \mu\text{g/g}\cdot\text{day}$ ), followed by Ni ( $\sim 105 \mu\text{g/g}\cdot\text{day}$ )

and Cr ( $\sim 34 \mu\text{g/g}\cdot\text{day}$ )—a release ranking obtained by other authors [39–41]. The low Cr corrosion rate did not follow its relative content in the alloy (Table 1), most likely due to its function: to improve the corrosion resistance by forming an external oxide layer. SEM micrographs (Figure 3) clearly showed a low-adherent external layer with multiple detachments in a “puzzlelike” morphology. The EDS elemental distribution maps showed that this top layer is mainly composed of O, Cr, and P. According to the passivation mechanisms in physiological conditions, the typical oxide layer on SS mainly includes Fe and Cr, with lower Ni content (typically in the inner layer region), and Mn and Mo, depending on the steel nominal composition [42,43]. Furthermore, the presence of P as phosphates in the passivation layers of metallic alloys, in physiological conditions, was reported in the literature [42] due to biocompatibility features. Yet, no pitting, crevices or other localized forms of corrosion were detected in the studied surfaces.

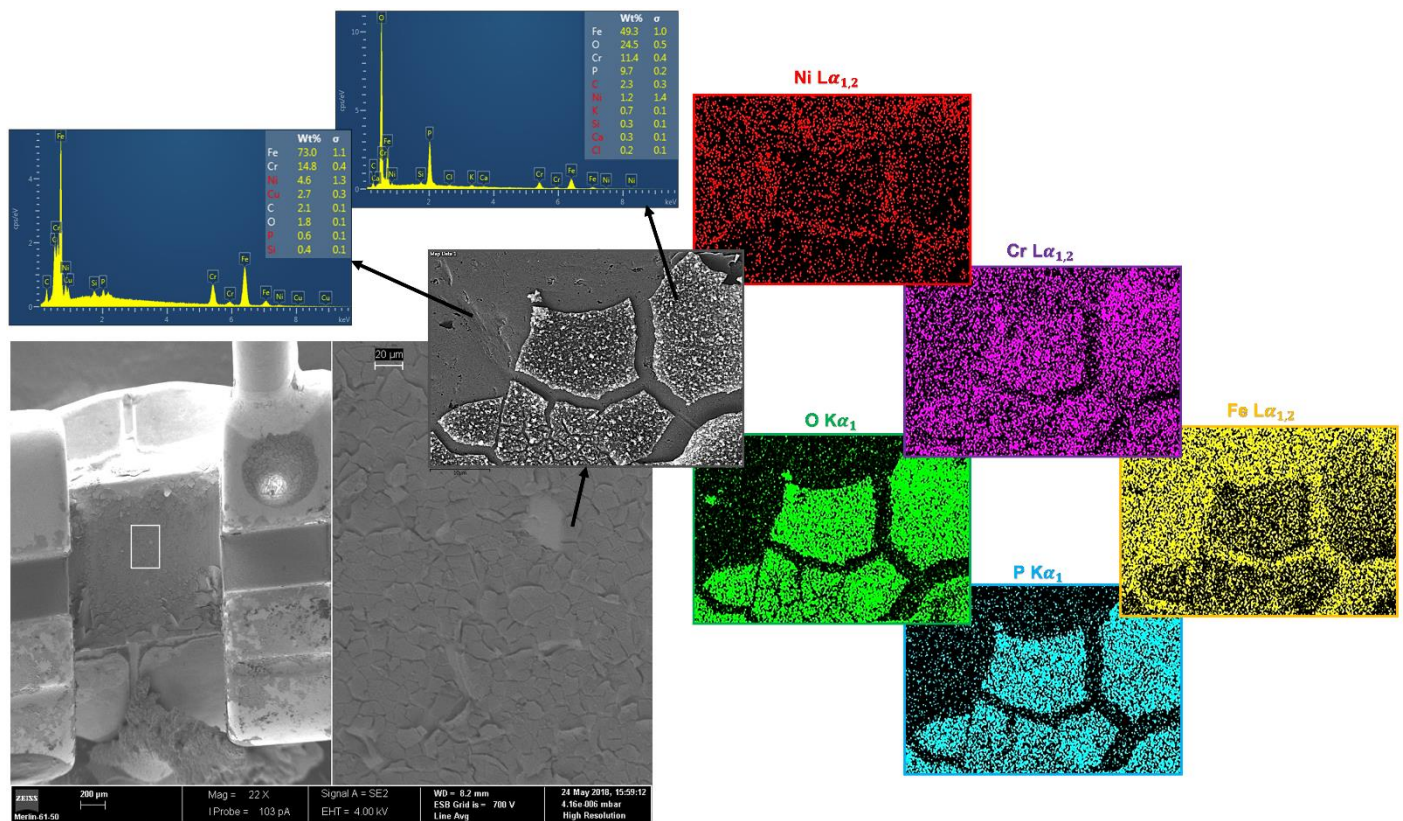


**Figure 3.** SEM surface micrographs and EDS analysis of brackets after the corrosion test at pH = 2.3.

As expected, considerably lower release rates were observed for the higher pH value of 6.8 ( $\sim 0.3$ , 0.03 and 0.005  $\mu\text{g/g}\cdot\text{day}$  of Fe, Cr, and Ni, respectively). In fact, brackets revealed no relevant surface morphological changes regarding its as-received state (figures not shown). A systematic literature review conducted by Mikulewicz and Chojnacka [44] also highlights the influence of the acid pH in the *in vitro* corrosion of SS appliances, finding a 30–50 times higher metal release in an acid environment than in more neutral solutions. Other authors of *in vitro* studies (not included in [44]) also reported the higher corrosion susceptibility and metallic release of various SS orthodontic components in more acid immersion solutions [45–49].

Tubes presented no signs of localized corrosion in either pH value. AISI630 SS is a precipitation-hardened alloy (martensitic structure) with high mechanical strength, high hardness, and excellent corrosion resistance, superior to the other austenitic SS studied grades. In fact, corrosion rates for Fe were almost 13 and 10 times lower than for brackets, and only traces of Ni were detected by ICP (Figure 2). Notice that this SS grade is the only one that presents the element Cu in the nominal composition (see Table 1), contributing

to the Ni equivalent effect. However, in the acidic saliva (pH = 2.3), SEM examination, coupled with EDS analysis (Figure 4) exposed traces of an outer layer with O, Cr, and P. Like in the case of brackets, this acidic condition influenced the adhesion of the passive layer. Notice that this “alveolar”, loose layer morphology contains higher P content (~13 wt.%) than in the case of brackets.

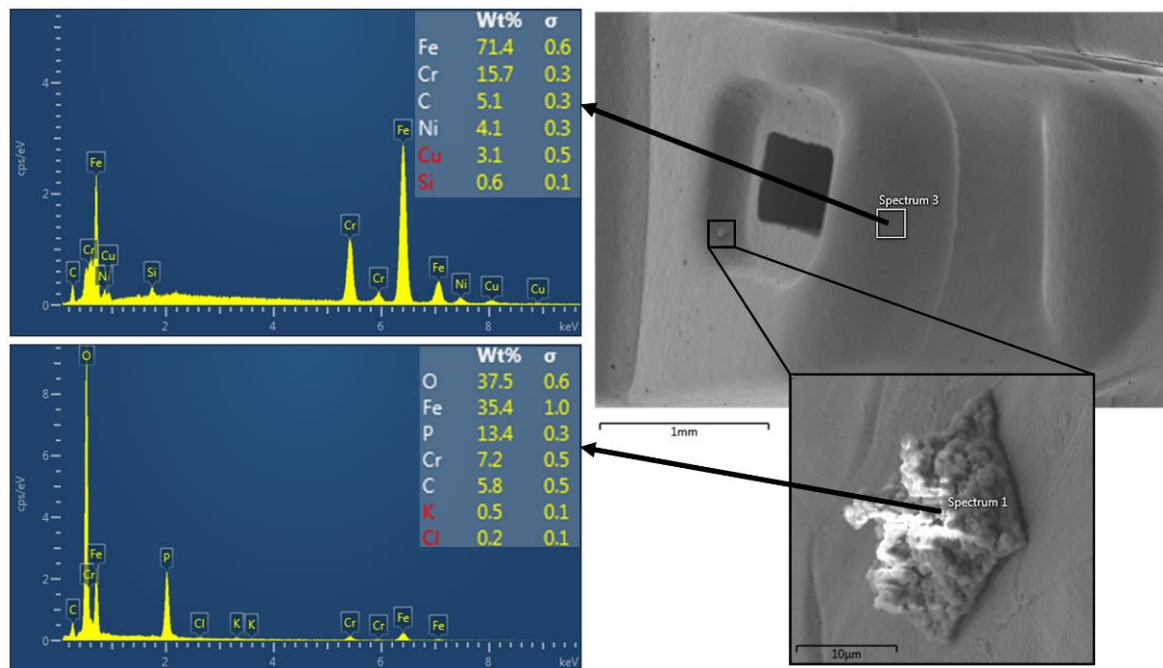


**Figure 4.** SEM surface micrographs and EDS analysis of tubes after the corrosion test at pH = 2.3.

Finally, the bands presented similar corrosion rates to those obtained for tubes (Figure 2). This behaviour may not be directly related to the corrosion resistance of bioalloy AISI305—with nominal composition similar to the AISI303 brackets—but decreased due to the presence of the AISI630 tube attached to the band (see Figure 1). Note that the bands are fixed to the molar teeth during the orthodontic treatment and have the function of fixing the archwires. Thus, it could be considered a dual orthodontic component.

Welding is a common procedure for manufacturing orthodontic pieces like brackets, bands, and tubes with more complex shapes [50]. However, welded pieces can greatly influence the release of metallic ions [41]. Soldered joints may promote galvanic corrosion and metallic ion release [5,6,51]. The outcomes can be harmful: Jacoby et al. [51], for instance, found a significant decrease in cell viability percentages in vitro after exposure to extracts of orthodontic bands containing Ag solder joints, whereas Freitas and colleagues [52] argue that “silver soldering used in orthodontics exhibits severe cell toxicity”.

The observation of the attached tube by SEM showed an O-based layer (Figure 5a,b) for both pH values. These layers are well-adherent but with similar morphological features and lower P content (~0.4 wt.%) than those on brackets and tubes (Figures 3 and 4). However, a careful analysis of the attached tube to the band (Figure 2) showed a worse corrosion behaviour at pH = 6.8 than brackets and tubes, suggesting that the influence of pH may not be the sole main contributor. In fact, Ag was detected in the top layer (Figure 5b), which is unexpected, since typical chemical compositions of SS alloys exclude this metallic element.

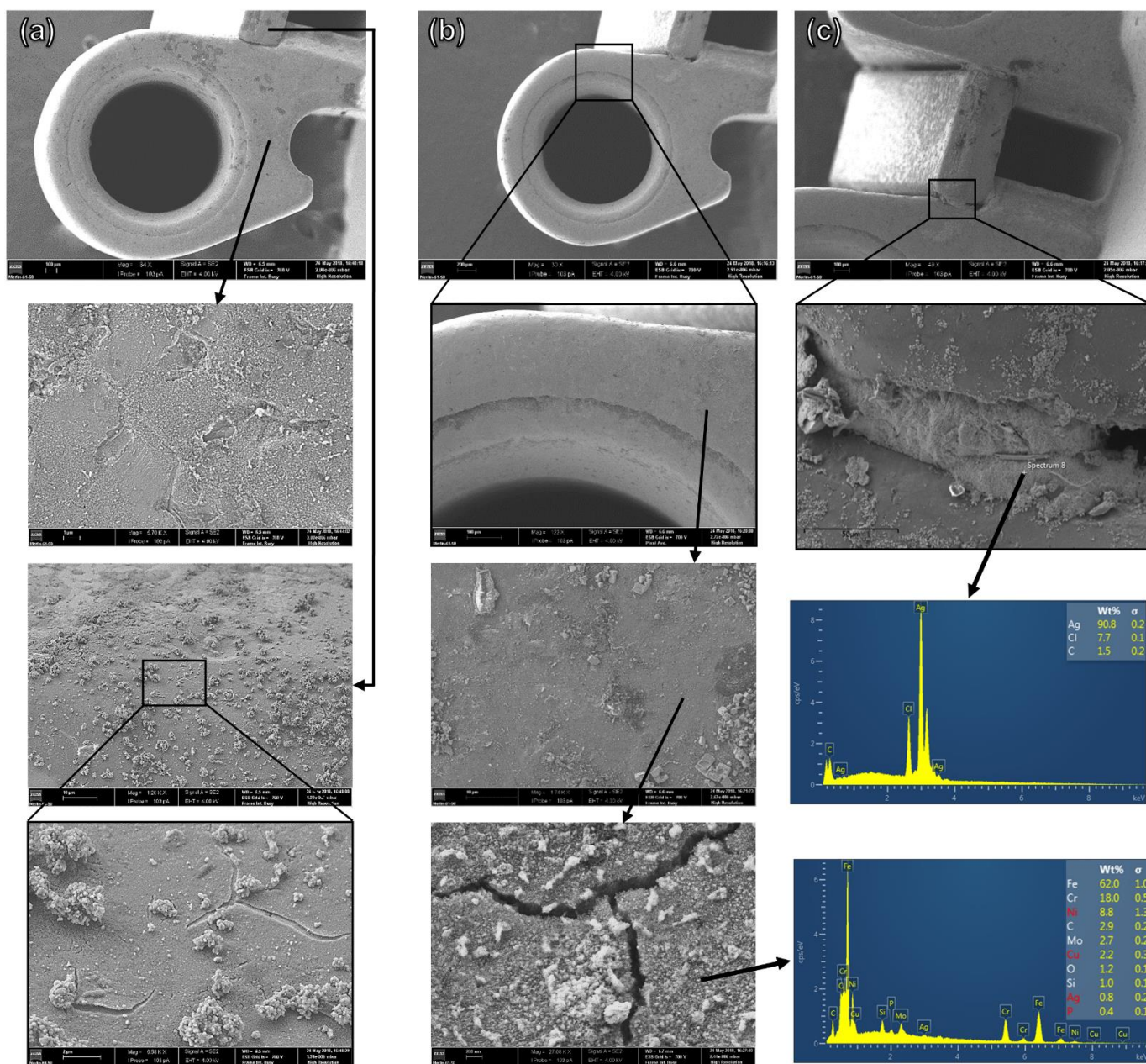


**Figure 5.** SEM surface micrographs and EDS analysis of the dental tube attached to the bands after the corrosion test at (a) pH = 6.8, and (b,c) pH = 2.3.

The Ag source was found near the adjacent rectangular orifice (Figure 5c): an Ag brazing material was used to weld a small metallic parallelepipedal to the main tube component. Additionally, Ag-containing particles of several shapes were spread over the surface of this component (Figure 5), preferentially located near the welded region. In this region, particles presented high Ag contents (as high as ~70 wt.%). This finding reinforces the influence of Ag-based welding in promoting corrosion of orthodontic components, as found by other authors [53,54].

To conclude the first part of this *in vitro* study, a simple calculation estimated the average daily amounts of metals released from a typical orthodontic appliance, composed of 20 brackets, 4 bands and 4 tubes, without considering NiTi or SS archwires—approximately 150, 55 and 307  $\mu\text{g}/\text{day}$ , respectively for Ni, Cr, and Fe.

Dietary studies conducted in different countries estimated a daily intake of Ni from food and drinking water of 100–300  $\mu\text{g}/\text{day}$ , while consumption of Ni-enriched foodstuffs



may increase this value up to 900  $\mu\text{g}/\text{day}$  [6,55]. Concerning Cr, an average daily intake of 280  $\mu\text{g}/\text{day}$  was estimated [6]. Finally, Fe is an essential element and is consumed daily in large quantities in the human diet, including in drinking water, and does not represent a risk to human health [56,57]. Average Cr and Ni releases obtained in this study are therefore within the daily intake levels and in accordance with several authors [40,45,46,58–61]. However, values are expected to peak in the first 1–2 weeks [40,41,60–62] of the orthodontic treatment. Besides, NiTi or SS archwires are used simultaneously with the studied components [2] and may contribute with more metal release into the oral cavity [39]. In a recent study [63], other authors found a significant increase in Ni concentration in the urine of patients undergoing orthodontic treatment, encouraging further research on bioaccumulation of this metal. Orthodontic appliances may be an additional source of potentially toxic elements that should not be disregarded [39], particularly for patients hypersensitive to Ni.

A possible path to improve the corrosion resistance of orthodontic metallic alloys is through protection of the surfaces with chemically inert coatings [20]. In this work, a-C:H-based coatings were sputter-deposited on an SS alloy with high Ni content, AISI310, to explore their potential as corrosion-protective films for orthodontic applications.

### 3.2. Sputtered a-C:H Coatings

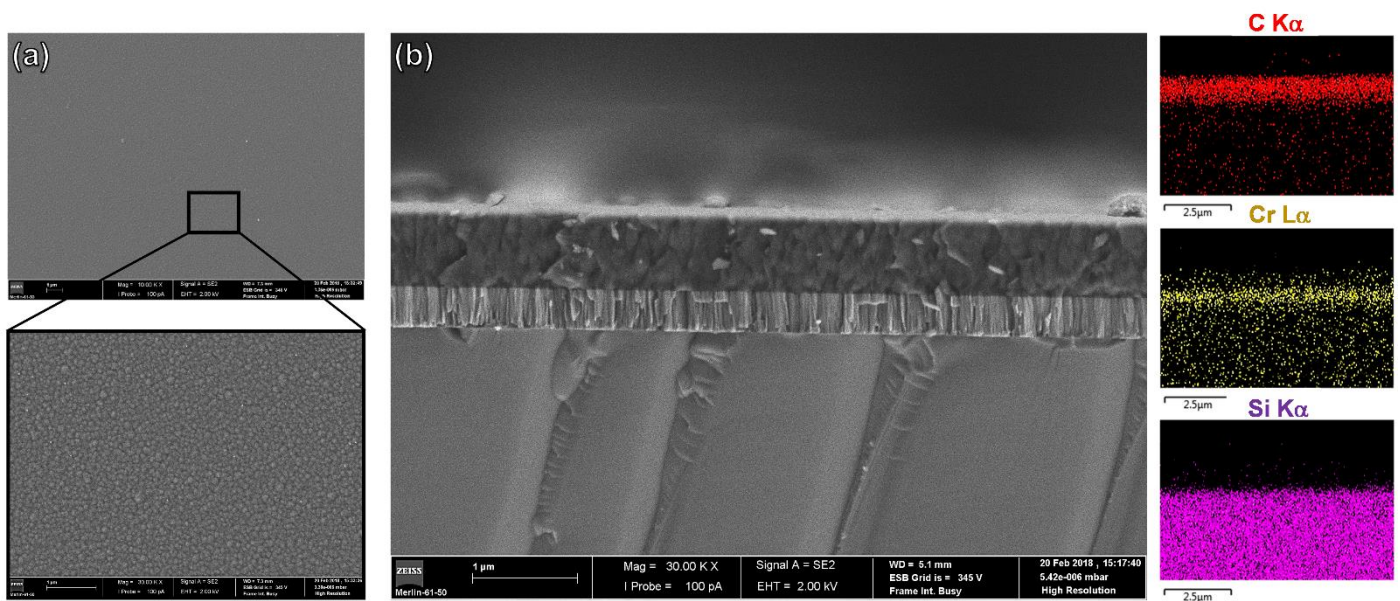
#### 3.2.1. Characterization Post-Deposition

Table 4 summarizes the main characteristics of the sputter-deposited a-C:H coatings, while Figure 6 displays the surface and cross-section micrographs and elemental distribution maps by SEM/EDS.

**Table 4.** Main characteristics of the a-C:H coatings before and after corrosion tests.

		As- Deposited	As-Immersed			
			7 Days		30 Days	
			pH 6.8	pH 2.3	pH 6.8	pH 2.3
Elemental composition [at.%]	C	96.4			96.7	96.7
	Cr	2.0	NE	NE	1.6	1.6
	Ar	1.6			1.7	1.7
Roughness [nm]	Ra	6.8	NE	NE	NE	8.7
Contact Angle [°]	-	56 ± 6	62 ± 12	59 ± 6	54 ± 2	54 ± 3
Nanohardness [GPa]	HB	22.7 ± 3.9	20.5 ± 1.9	17.5 ± 1	23.7 ± 1.9	20.5 ± 2.0
Raman bonding configuration	G band [ $\text{cm}^{-1}$ ]	1549	1550	1548	1546	1546
	ID/IG ratio	0.45	0.45	0.46	0.45	0.46
	C-C sp <sup>3</sup> [%]	39	39	40	41	41
FTIR analysis	C-H sp <sup>2</sup> /sp <sup>3</sup> ratio	0.31	0.31	0.19	0.16	0.16

Concerning the coatings' morphology (Figure 6), SEM micrographs revealed a C-based top layer (~770 nm) with a typical *cauliflower*-like surface morphology [31,33,64–66] deposited on a well-adherent Cr-based interlayer. No preferential growth direction of the a-C:H coating was detected, in contrast with the well-defined columnar morphology of the buffer/adhesion layer (~380 nm). The good elemental chemical homogeneity is corroborated by the EDS analysis, as shown in Figure 6. In agreement with previous results [31], a small Ar contamination was detected due to the carrier-gas effect during the films' formation.



**Figure 6.** SEM (a) Surface and (b) cross-section micrographs of the a-C:H coating deposited on Si substrates and the corresponding EDS elemental distribution maps.

Visible Raman and FTIR spectroscopies were complementarily employed to evaluate the a-C:H chemical properties, namely the  $sp^2/sp^3$  C–C bindings and the H-bonded content. Typical Raman spectra presenting the two broadened D and G bands were acquired (Figure 7a). Successful peak fitting allowed for the location of the graphitic signature of C ( $sp^2$  hybridization G band) at  $\sim 1549\text{ cm}^{-1}$ , while the disorder clusters of hexagonal sheets of C ( $sp^2$  hybridization D bands) were found at  $\sim 1411\text{ cm}^{-1}$ .

The absence of the notorious Raman photoluminescence background suggests an H content in the studied coating below  $\sim 25\text{ at.}\%$  [25,31,38,67,68]. In fact, by using a nanohardness of 22.7 GPa in Equation (3), an H content of  $\sim 23\text{ at.}\%$  was estimated. Together with the obtained  $I_D/I_G$  ratio of  $\sim 0.45$  (Table 4), these results are in perfect agreement with those obtained by other authors [25]. The  $sp^2$  C–C hybridization dominates the structure of the coatings, as the estimated  $sp^3$  C–C fraction was  $\sim 39\%$  from Equation (1). Thus, based upon the a-C:H materials classification [25,69]—established in the ternary  $sp^2$ - $sp^3$ -H diagram—the sputter-deposited a-C:5H coatings in this study can be considered a diamond-like a-C:H (DLCH) coating. DLCH coatings are characterized by high hardness values, up to around 20 GPa, and a carbon  $sp^3$  hybridization range of 40–60% [70], corroborating the data obtained from the a-C:5H films.

Following other authors [21,69] who claimed that the main effect of H in an a-C:H film is to modify the C–C bonding not by increasing their fraction but by terminating the sites of double bonding of carbon as C–H<sub>x</sub> ( $x = 1, 2, 3$ ), FTIR analyses were performed. As can be seen in Figure 7b, the wide, broad band centred at  $\sim 2900\text{ cm}^{-1}$ , whose Gaussian peak fitting results in nine superimposed peaks, can be assigned to the stretching modes of both  $sp^2$ - and  $sp^3$ -C–H<sub>x</sub> bonds in the range of  $\sim 2800$ – $3300\text{ cm}^{-1}$  [21]. Table 5 lists the FTIR peaks, identified by an index, correlating their positions with their assignments. While peaks 1 to 4 are assigned to  $sp^2$ -CH<sub>x</sub> bonds, peaks 5 to 9 are due to  $sp^3$ -CH<sub>x</sub> bonds. Using Equation (2) and the relative FTIR peak areas (Table 5), a predominance of  $sp^3$ -bonded H to C atoms over  $sp^2$  C–H bonds was estimated:  $sp^2/sp^3 \sim 0.31$ . This means that hydrogen is preferentially bonded to  $sp^3$ -hybridized C atoms [71].

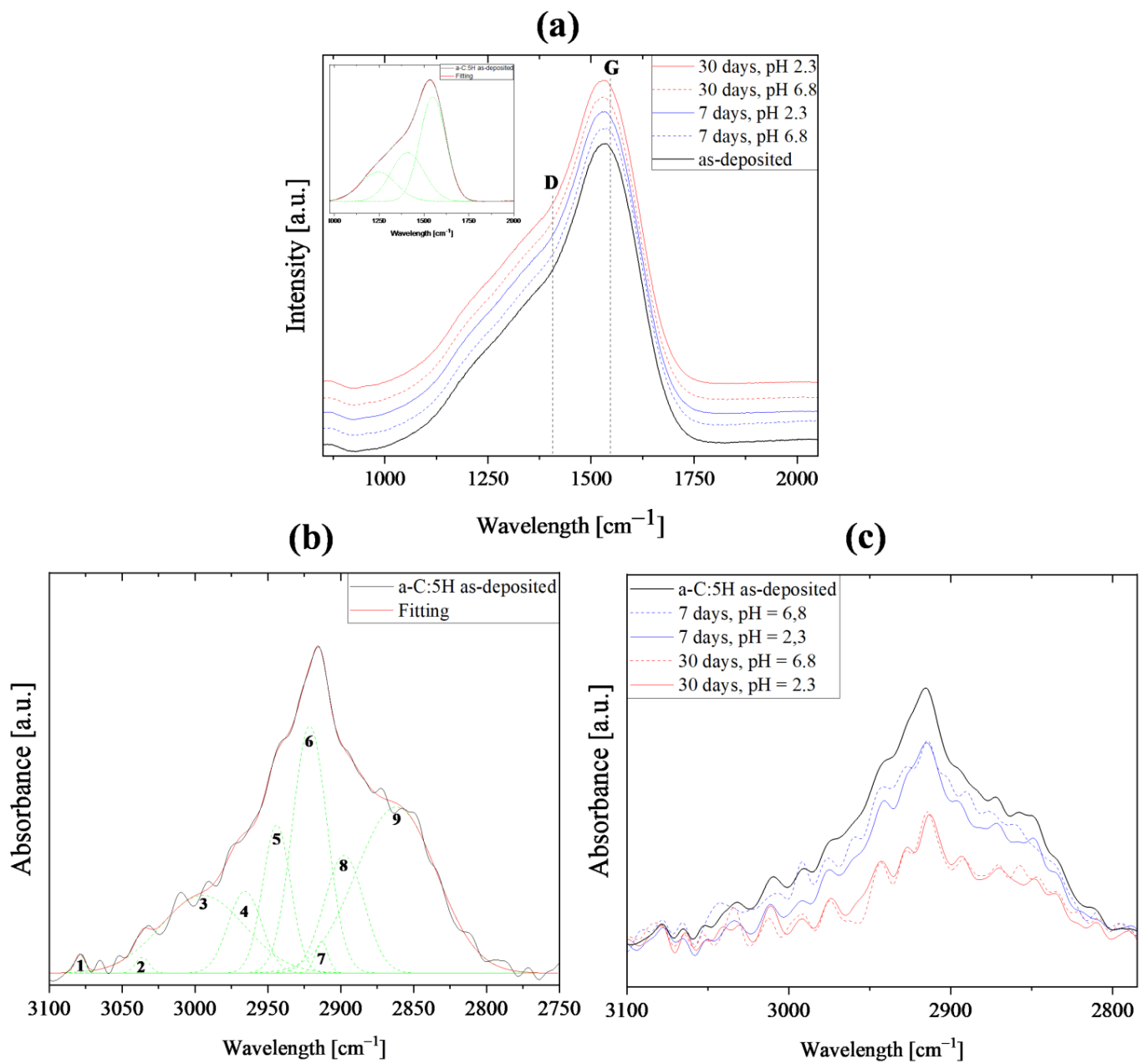


**Figure 7.** Structural characterization of the a-C:5H coatings before and after the corrosion tests by (a) visible Raman (inset: Gaussian fitting result of the as-deposited a-C:H coating); and (b,c) FTIR spectroscopy.

### 3.2.2. Characterization Post-Corrosion Tests

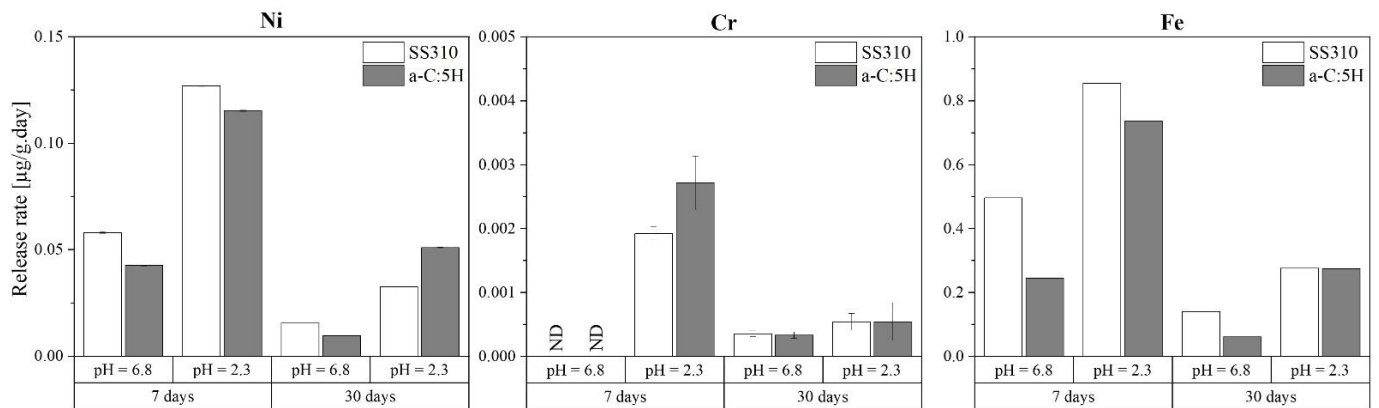
The ICP-OES data for both coated and uncoated SS310 samples (Table 3) are displayed in Figure 8 as metal release rates. Three main conclusions were clear from the data:

1. Release rates increased with decreasing pH values of the saliva;
2. Release rates decreased with increasing immersion times;
3. Ni release rates were higher than those of Cr for both reference SS310 and a-C:5H samples.

**Table 5.** FTIR peak fitting results of vibrational frequency assignments of as-deposited and as-immersed a-C:H coatings: peak positions ( $Pos_i$ ) and areas ( $A_i$ ).

Index (i)	Peak Assignment [21] Configuration	Position ( $cm^{-1}$ )	As-dep.		7 Days pH = 6.8		7 Days pH = 2.3		30 Days pH = 6.8		30 Days pH = 2.3	
			$Pos_i$	$A_i$	$Pos_i$	$A_i$	$Pos_i$	$A_i$	$Pos_i$	$A_i$	$Pos_i$	$A_i$
			( $cm^{-1}$ )	( $cm^{-1}$ )	(a.u.)	( $cm^{-1}$ )	(a.u.)	( $cm^{-1}$ )	(a.u.)	( $cm^{-1}$ )	(a.u.)	( $cm^{-1}$ )
1	CH <sub>2</sub> -sp <sup>2</sup> (A)	3085	3079	0.03	3080	0.06	3078	0.05	3082	0.04	3080	0.03
2	CH-sp <sup>2</sup>	3035	3036	0.03	3044	0.06	3036	0.04	3035	0.06	3037	0.04
3	CH-sp <sup>2</sup> (S)	2990–3000	2995	0.94	2997	0.85	2997	0.46	2994	0.16	3004	0.19
4	CH <sub>2</sub> -sp <sup>2</sup> (S)	2975	2966	0.39	2974	0.25	2973	0.21	2974	0.07	2974	0.09
5	CH <sub>3</sub> -sp <sup>3</sup> (A)	2955	2944	0.60	2948	0.43	2949	0.50	2943	0.28	2945	0.45
6	CH <sub>2</sub> -sp <sup>3</sup> (A)	2920	2921	1.23	2924	1.17	2922	1.17	2919	0.48	2918	0.46
7	CH-sp <sup>3</sup>	2920	2913	0.06	2914	0.05	2915	0.09	2914	0.08	2912	0.05
8	CH <sub>3</sub> -sp <sup>3</sup> (S)	2885	2898	0.67	2897	0.66	2897	0.51	2895	0.22	2897	0.30
9	CH <sub>2</sub> -sp <sup>3</sup> (S)	2855	2862	1.93	2861	1.66	2860	1.63	2860	1.06	2860	0.94

A: Antisymmetric stretching vibration; S: Symmetric stretching vibration.

**Figure 8.** Average release rates of Ni, Cr, and Fe of SS310 and a-C:5H samples. ND: not detected.

After the 30-day immersion corrosion test in the artificial saliva with pH = 2.3, SEM surface analysis revealed pitting corrosion on the SS310 uncoated samples (Figure 9), which were absent at pH = 6.8. Indeed, SS, as all Fe alloys, is known to be susceptible to pitting corrosion, especially in chloride-containing solutions [43,72,73]. This is a localized metal dissolution reaction, which is nucleated at the external passive film by the presence of defects such as crevices, pores, inclusions, etc. The reaction progress requires that the environment inside the pit be able to maintain the continuous active dissolution state at the pitting surface. Two main constituents, H<sup>+</sup> and Cl<sup>-</sup>, are involved: H<sup>+</sup> is derived from the hydrolysis of metal cations, and Cl<sup>-</sup> (in solution) migrates into the pit to balance the charge and maintain the electroneutrality.

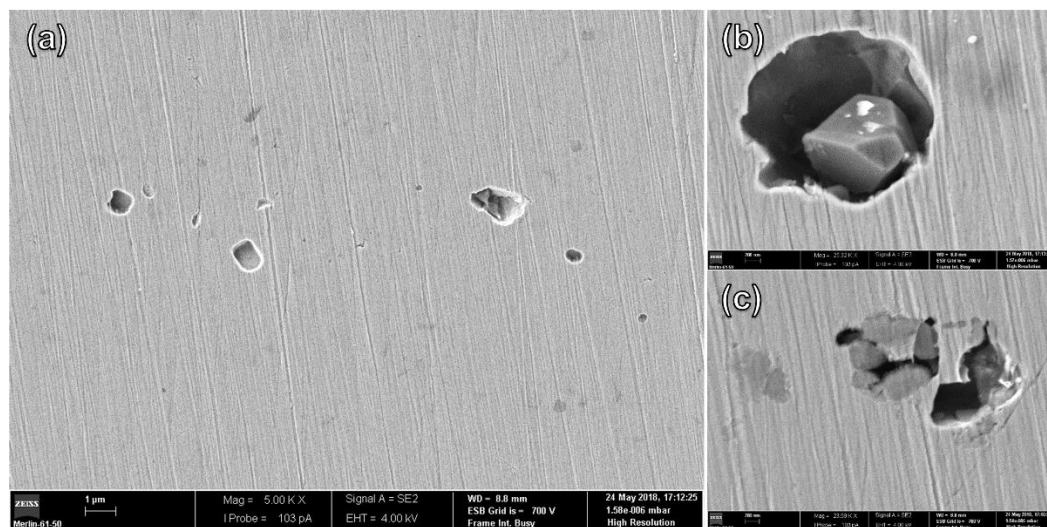


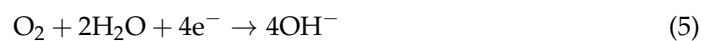
**Figure 9.** (a) SEM surface micrographs of SS310 reference samples after the corrosion test at pH = 2.3; (b,c) detailed views of pit morphologies.

The pitting corrosion process can be summarized as follows [73]:

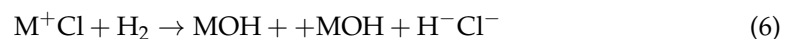
1. «Anodic site formation is the first stage in pitting where the passive protective layer on the surface of the metal is destroyed. The destruction of the protective film may be done chemically or mechanically.



It is then balanced by reacting oxygen on the adjacent surface at the Cathode



2. The continuous dissolution of metal results to the accumulation of outrageous positive ions ( $M^+$ ) at the anodic zone. This is a self-stimulating and self-propagating process. Neutralization of charges is sustained by the negative ions (anions), like chloride which comes from the electrolyte (using seawater as sample).



The positive charges are kept neutralized by the hydroxyl ions ( $OH^-$ ) through hydrolysis process.

3. Repassivation is prevented by the presence of hydrogen ion and chloride content. This process produces free acid while the value of pH at the base of the pit is significantly decreased (1.5–1.0).
4. The rate of migration of chloride ion increases with dissolution rate at the anode. This makes the reaction to be time dependent and leading to the formation of more  $M^+Cl^-$  and the hydrolysis of  $H^+Cl^-$ .
5. This process go on till the point of perforation of the metal. This is an autocatalytic process which advances with time leading to more metal dissolution.
6. The metal finally perforate thereby causes the termination of the process.»

Hence, the increase in the  $H^+$  concentration (lowering pH from 6.8 to 2.3) leads to a pit increase in the  $Cl^-$  ions, which intensifies the local progression reaction and further decreases the local pH value.

In fact, the corrosion resistance of SS310 in acidic saliva, for both immersion times, was low for all evaluated metallic elements (Table 3 and Figure 8). As expected, Fe ranks first, followed by Ni, in agreement with the results from the real orthodontic components.

A noticeable behaviour is the higher release rate of all elements after 7 days than after 30 days: the initial “burst” release precedes the beginning of the spontaneous passivation process, i.e., the formation of a Cr-based oxide layer. Over time, surface oxide formation progresses and a decrease in metal release rates is expected [40,41,58,60–62]. The passivation mechanism seemed to reach a thermodynamic equilibrium, therefore stabilizing the release rates.

Unexpectedly, some abnormal profiles were detected for a-C:H coatings (Figure 8). While the release rates in saliva with pH = 6.8 were always lower than those from SS310, the same did not always occur in the more acidic saliva. Right after 7 days of immersion, the Cr release rate from a-C:5H was ~40% higher than that from uncoated SS310 but was similar at day 30. Ni release from coatings was ~10% lower than SS310 after 7 days but ~55% higher after 30 days. Finally, Fe release was ~15% lower and similar to SS310 after 7 and 30 days, respectively. This logic-defying behaviour exceeded the single influence of pH on the samples, especially if the abovementioned overall inertness of the a-C:H coating is considered.

Fe remains the main released element, followed by Ni. At day 7, more than the absence of a passivation equilibrium, a corrosion-promoting mechanism was taking place: Cr was released at a higher rate than from uncoated SS310. As time progressed, Cr (and possibly Fe) from the alloy seemed to participate in the passivation phenomenon, explaining the similar release rates from SS310 and a-C:5H at day 30, contrary to Ni, which leached into the saliva.

The SEM/EDS analysis seems to contradict the ICP-OES data and evidences a clear stability of the top a-C:5H as an anticorrosive layer in all study conditions: no segregation, metallic inclusion, delamination, or detachments were detected (Figure 10). In fact, the surface polishing “linear defects”—almost null for coatings deposited on the Si wafers (Figure 6)—were potential diffusion paths for saliva to reach the coating/substrate interface, and thus promoting corrosion; however, the morphology looked unchanged, with no observable chemical composition variation by EDS analysis, regardless the saliva pH value. The good adhesion of this coating to the SS substrate, promoted by the Cr-based interlayer, avoided detachment from the SS substrate.

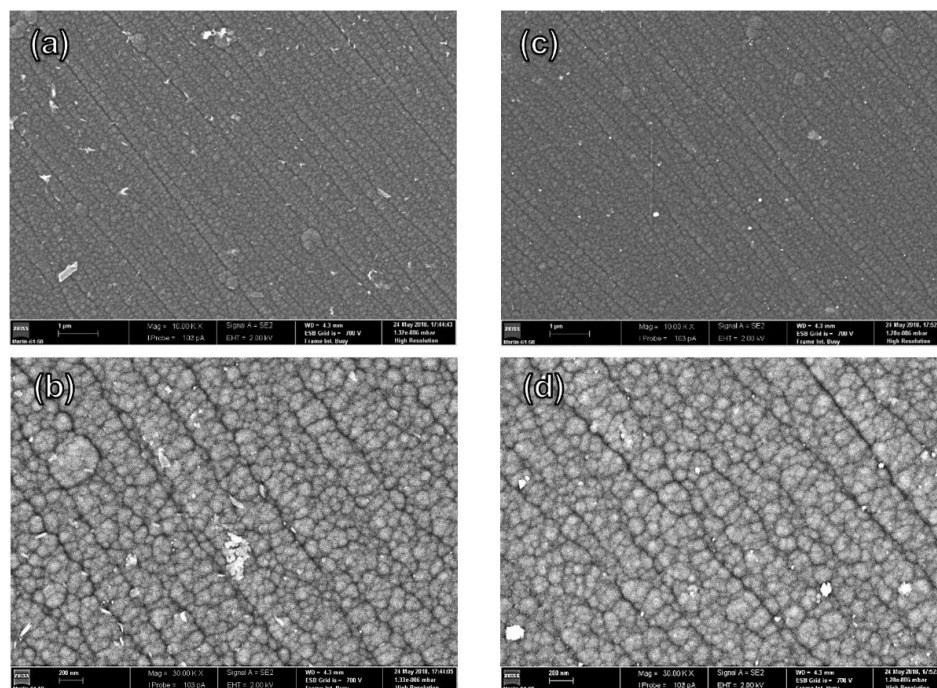


**Figure 10.** SEM surface micrographs of the a-C:5H coatings deposited on SS310 substrates after the corrosion tests at (a,b) pH = 6.8; and (c,d) pH = 2.3.

Static contact angle values obtained with water are compiled in Table 4. The as-deposited a-C:5H surface presented a slightly higher water contact angle value ( $\sim 56^\circ$ ) than the only-polished SS310 substrate ( $\sim 53^\circ$ ). Such values suggest that these surfaces are hydrophilic [74]. However, when the a-C:5H coating was deposited on Si substrates, a water contact angle of  $71^\circ \pm 3^\circ$  was obtained, comparable to those obtained by several authors on sputtered DLC coatings [21,31,75–77]. Defects on the SS surface from polishing seemed the cause of this divergence: during coating growth, these “linear” features influence the final coating-surface morphology (roughness), and therefore, the wettability. Nonetheless, a-C:5H coating presented a low Ra:  $\sim 7$  nm (Table 4).

After the *in vitro* corrosion tests, no significant variations on static contact angles were detected for all immersion conditions when compared with the as-deposited state (Table 4). While pitting corrosion occurred on SS10 samples, its extent seemed insufficient to cause major wettability changes. On the other hand, a-C:5H coatings, which conserved both chemical and morphological characteristics, also maintained the as-deposited hydrophilic character. Moreover, Ra values of the coatings registered only a minor variation after 30 days at pH = 2.3 (Table 4), which seemed negligible:  $\sim 7$  and 9 nm before and after immersion, respectively.

Both Raman and FTIR analyses corroborate the chemical structure stability of the coatings under study at oral physiological pH values, as well as in acid conditions (Figure 7). The Raman spectra evolution, shown in Figure 7a, presented unquestionably similar features, resulting in almost invariable G and D peak positions,  $I_D/I_G$  ratios, and  $sp^3$  content (Table 4) regarding the as-deposited state. In addition, the mechanical behaviour, referenced by nanohardness, was preserved after immersion in artificial saliva; that is,  $\sim 20$  GPa.

FTIR results confirmed the prevalence of  $sp^3$  C-H bonds after the corrosion tests, with a variation that was reflected in the  $sp^2/sp^3$  variation: this ratio, which relates the area of peaks 1 to 4 (C-H  $sp^2$ ) and 5 to 9 (C-H  $sp^3$ ), decreased in time, regardless the pH value (Table 4 and Figure 7b). Note, however, that the intensity of the spectra decreases in the studied region ( $2800\text{--}3100\text{ cm}^{-1}$ ). The total area under this spectral region is a relative measure for the content of bonded H in the a-C:H coatings, which may indicate a small decrease in bonded H to C atoms over time [71].

The inertness of a-C:H coatings was therefore supported, even for the longer immersion period in the acidic artificial saliva, suggesting their potential use as protective coatings for orthodontic applications.

The simultaneous presence of this inert layer on the substrates and similar or even higher release rates of metallic elements is, however, difficult to explain. Similar results were also obtained in a previous research work [31]. A recent study [78] may have provided the answer to this enigma: the authors highlighted the crucial role of metallic-based interlayers in increasing overall corrosion susceptibility, due to the formation of galvanic cells, particularly if Cr-C based interlayers are used. Therefore, the corrosion of the coatings in the present study should be due to the presence of the Cr-based interlayer and not to the highly stable a-C:H coating. This may also explain the main source of Cr in the first 7 days: the buffer interlayer. Such findings illustrate the crucial importance of the interface between metal substrates/coating systems when C-based coatings are to be considered for orthodontic applications. Indeed, most authors that found a significant *in vitro* decrease in metal release from DLC-coated samples did not report the use of adhesion-promoting interlayers [79,80].

From the corrosion behaviour at pH = 2.3 of both orthodontic components and either coated or uncoated SS310 samples, three conclusions arise from an overall discussion of the results:

1. Brackets released substantially more Fe, Ni, and Cr than any other studied samples;
2. Both uncoated and a-C:H-coated SS310 samples released significantly less Cr and Fe than real orthodontic components; and
3. Ni release rates were lower from tubes and bands than from SS310 and a-C:5H samples at day 7 (less than 50%) but similar (a-C:5H) or higher (SS310) at day 30.

The explanation for these corrosion profiles might lie in the use of different SS grades (with different corrosion resistance) and/or manufacturers [62,81]. Note that besides higher Ni, SS310 presents higher Cr content than the steel grades of the orthodontic components (Table 1). The lack of clear corrosion signs on the surface of orthodontic pieces, especially in the case of brackets, may be a consequence of the complex surface geometry, which may have camouflaged signs of localized corrosion forms that clearly appeared on the surface of SS310.

The direct comparison of this study with other *in vitro* research works is difficult due to the multiple methodologies with different constituents (e.g., materials, manufacturers, immersion solutions), even when assessing the *in vitro* cytotoxicity [14]. Therefore, this study focused on comparing metallic ion release trends rather than quantities, while assessing the potential use of a-C:H coatings as diffusion barriers for SS bioalloys.

Further ongoing work centres on optimizing overall coating production by replacing the interlayer with other types of materials and architectures. Moreover, *in vitro* cytotoxicity tests and microbiological assays with representative oral bacteria will soon be performed to ascertain their influence on the sputter-deposited a-C:H coatings.

#### 4. Conclusions

The present *in vitro* research work is divided into two sections and assessed the saliva pH effect on both orthodontic components and the sputter-deposited a-C:H coatings.

In the first part, real SS brackets, tubes, and bands were characterized before and after a 30-day *in vitro* corrosion test with Fusayama-Meyer artificial saliva, and released Ni, Cr, and Fe were quantified. The results showed that: (i) salivary pH clearly influenced corrosion behaviour; (ii) brackets were, by far, the main source of metallic ions into the saliva; (iii) Ag welding found on bands may have influenced the corrosion behaviour, regardless the pH value of the saliva; (iv) released Ni was within daily dietary intake values. Orthodontic appliances may be an additional source of potentially toxic elements that should not be disregarded.

In the second part, hydrogenated amorphous carbon films were successfully deposited over SS310 by reactive magnetron sputtering, with a Cr-based adhesion promoting interlayer. The a-C:H top layer was found in the hard regime (over 20 GPa) and classified as DLCH. While AISI310 substrates presented clear signs of pitting corrosion in acidic conditions, the a-C:H conserved the chemical, mechanical, and structural inertness, as well as the anticorrosion ability. The well-known stability of amorphous C-based materials was therefore verified. However, leaching of metallic ions from a-C:H coatings was higher than from SS310. This unexpected result was attributed to galvanic effects between dissimilar materials: Cr-based interlayer and SS substrates.

**Author Contributions:** Conceptualization, C.S.L. and A.C.S.; data curation, A.F.; formal analysis, A.F.; funding acquisition, A.F.; investigation, A.F. and M.E.; methodology, C.S.L. and A.C.S.; project administration, C.S.L. and A.C.S.; resources, C.S.L., A.C.S. and M.E.; supervision, C.S.L. and A.C.S.; validation, C.S.L., A.F. and A.C.S.; visualization, A.F. and M.E.; writing—original draft, A.F.; writing—review and editing, C.S.L. and A.C.S. All authors have read and agreed to the published version of the manuscript.

**Funding:** This research is sponsored by national funds through FCT—Fundação para a Ciência e a Tecnologia, through PhD Grant SFRH/BD/143905/2019 attributed to A.F.

**Institutional Review Board Statement:** Not applicable.

**Informed Consent Statement:** Not applicable.

**Data Availability Statement:** Not applicable.

**Acknowledgments:** This research is sponsored by national funds through FCT—Fundação para a Ciência e a Tecnologia, under the project UIDB/00285/2020.

**Conflicts of Interest:** The authors declare no conflict of interest.



## References

1. European Commission Regulation (EC) 1907/2006 of the European Parliament and of the Council of 18 December 2006-REACH. Available online: <http://eur-lex.europa.eu/legal-content/EN/TXT/PDF/?uri=CELEX:32006R1907&from=en>. (accessed on 25 August 2021).
2. Proffit, W.R.; Fields, H.W.; Sarver, D.M.; Ackerman, J.L. Contemporary orthodontic appliances. In *Contemporary Orthodontics*; Elsevier: Amsterdam, The Netherlands, 2012; pp. 347–389. ISBN 978032308317.
3. Abdallah, M.-N.; Lou, T.; Retrouvey, J.-M.; Suri, S. Biomaterials used in orthodontics: Brackets, archwires, and clear aligners. In *Advanced Dental Biomaterials*; Khurshid, Z., Najeeb, S., Zafar, M.S., Sefat, F.B.T.-A.D.B., Eds.; Elsevier: Amsterdam, The Netherlands, 2019; pp. 541–579. ISBN 978-0-08-102476-8.
4. Tsihlaki, A.; Chin, S.Y.; Pandis, N.; Fleming, P.S. How long does treatment with fixed orthodontic appliances last? A systematic review. *Am. J. Orthod. Dentofac. Orthop.* **2016**, *149*, 308–318. [[CrossRef](#)]
5. Chaturvedi, T.P.; Upadhyay, S.N. An overview of orthodontic material degradation in oral cavity. *Indian J. Dent. Res.* **2010**, *21*, 275–284. [[CrossRef](#)] [[PubMed](#)]
6. House, K.; Sernetz, F.; Dymock, D.; Sandy, J.R.; Ireland, A.J. Corrosion of orthodontic appliances—should we care? *Am. J. Orthod. Dentofac. Orthop.* **2008**, *133*, 584–592. [[CrossRef](#)] [[PubMed](#)]
7. Eliades, T.; Athanasiou, A.E. In vivo aging of orthodontic alloys: Implications for corrosion potential, nickel release, and biocompatibility. *Angle Orthod.* **2002**, *72*, 222–237. [[PubMed](#)]
8. Dwivedi, A.; Tikku, T.; Khanna, R.; Maurya, R.P.; Verma, G.; Murthy, R.C. Release of nickel and chromium ions in the saliva of patients with fixed orthodontic appliance: An in-vivo study. *Natl. J. Maxillofac. Surg.* **2015**, *6*, 62–66. [[CrossRef](#)]
9. Mystkowska, J.; Niemirowicz-Laskowska, K.; Łysik, D.; Tokajuk, G.; Dąbrowski, J.R.; Bucki, R. The role of oral cavity biofilm on metallic biomaterial surface destruction—corrosion and friction aspects. *Int. J. Mol. Sci.* **2018**, *19*, 743. [[CrossRef](#)] [[PubMed](#)]
10. Choi, J.E.; Lyons, K.M.; Kieser, J.A.; Waddell, N.J. Diurnal variation of intraoral pH and temperature. *BDJ Open* **2017**, *3*, 17015. [[CrossRef](#)]
11. Sandin, B.; Chorot, P. Changes in skin, salivary, and urinary pH as indicators of anxiety level in humans. *Psychophysiology* **1985**, *22*, 226–230. [[CrossRef](#)] [[PubMed](#)]
12. IARC (International Agency for Research on Cancer). Nickel and nickel compounds. *IARC Monogr. Eval. Carcinog. Risks Hum.* **2011**, *100*, 169–218. [[CrossRef](#)]
13. Agarwal, P.; Upadhyay, U.; Tandon, R.; Kumar, S. Nickel allergy and orthodontics. *Asian J. Oral Heal. Allied Sci.* **2011**, *1*, 61–63.
14. Martín-Cameán, A.; Jos, Á.; Mellado-García, P.; Iglesias-Linares, A.; Solano, E.; Cameán, A.M. In vitro and in vivo evidence of the cytotoxic and genotoxic effects of metal ions released by orthodontic appliances: A review. *Environ. Toxicol. Pharmacol.* **2015**, *40*, 86–113. [[CrossRef](#)] [[PubMed](#)]
15. Genchi, G.; Carocci, A.; Lauria, G.; Sinicropi, M.S.; Catalano, A. Nickel: Human health and environmental toxicology. *Int. J. Environ. Res. Public Health* **2020**, *17*, 679. [[CrossRef](#)]
16. Dunlap, C.L.; Vincent, S.K.; Barker, B.F. Allergic reaction to orthodontic wire: Report of case. *J. Am. Dent. Assoc.* **1989**, *118*, 449–450. [[CrossRef](#)] [[PubMed](#)]
17. Kolokitha, O.E.; Chatzistavrou, E. A severe reaction to Ni-containing orthodontic appliances. *Angle Orthod.* **2009**, *79*, 186–192. [[CrossRef](#)]
18. Ellis, P.E.; Benson, P.E. Potential Hazards of orthodontic treatment—What your patient should know. *Dent. Update* **2002**, *29*, 492–496. [[CrossRef](#)] [[PubMed](#)]
19. Russell, J.S. Current products and practice: Aesthetic orthodontic brackets. *J. Orthod.* **2005**, *32*, 146–163. [[CrossRef](#)] [[PubMed](#)]
20. Arango, S.; Peláez-Vargas, A.; García, C. Coating and surface treatments on orthodontic metallic materials. *Coatings* **2013**, *3*, 1–15. [[CrossRef](#)]
21. Robertson, J. Diamond-like amorphous carbon. *Mater. Sci. Eng. R Rep.* **2002**, *37*, 129–281. [[CrossRef](#)]
22. Vetter, J. 60years of DLC coatings: Historical highlights and technical review of cathodic arc processes to synthesize various DLC types, and their evolution for industrial applications. *Surf. Coat. Technol.* **2014**, *257*, 213–240. [[CrossRef](#)]
23. Zahid, R.; Masjuki, H.H.; Varman, M.; Kalam, M.A.; Mufti, R.A.; Zulkifli, N.W.B.M.; Gulzar, M.; Azman, S.S.B.N. Influence of intrinsic and extrinsic conditions on the tribological characteristics of diamond-like carbon coatings: A review. *J. Mater. Res.* **2016**, *31*, 1814–1836. [[CrossRef](#)]
24. Ohgoe, Y.; Hirakuri, K.K.; Saitoh, H.; Nakahigashi, T.; Ohtake, N.; Hirata, A.; Kanda, K.; Hiratsuka, M.; Fukui, Y. Classification of DLC films in terms of biological response. *Surf. Coat. Technol.* **2012**, *207*, 350–354. [[CrossRef](#)]
25. Casiraghi, C.; Ferrari, A.C.; Robertson, J. Raman spectroscopy of hydrogenated amorphous carbons. *Phys. Rev. B* **2005**, *72*, 085401. [[CrossRef](#)]
26. Hauert, R.; Thorwarth, K.; Thorwarth, G. An overview on diamond-like carbon coatings in medical applications. *Surf. Coat. Technol.* **2013**, *233*, 119–130. [[CrossRef](#)]
27. Love, C.A.; Cook, R.B.; Harvey, T.J.; Dearnley, P.A.; Wood, R.J.K. Diamond like carbon coatings for potential application in biological implants—A review. *Tribol. Int.* **2013**, *63*, 141–150. [[CrossRef](#)]
28. Kang, T.; Huang, S.-Y.; Huang, J.-J.; Li, Q.-H.; Diao, D.-F.; Duan, Y.-Z. The effects of diamond-like carbon films on fretting wear behavior of orthodontic archwire-bracket contacts. *J. Nanosci. Nanotechnol.* **2015**, *15*, 4641–4647. [[CrossRef](#)]

29. Muguruma, T.; Iijima, M.; Kawaguchi, M.; Mizoguchi, I. Effects of sp<sup>2</sup>/sp<sup>3</sup> ratio and hydrogen content on in vitro bending and frictional performance of DLC-coated orthodontic stainless steels. *Coatings* **2018**, *8*, 199. [[CrossRef](#)]
30. Akaïke, S.; Kobayashi, D.; Aono, Y.; Hiratsuka, M.; Hirata, A.; Hayakawa, T.; Nakamura, Y. Relationship between static friction and surface wettability of orthodontic brackets coated with diamond-like carbon (DLC), fluorine- or silicone-doped DLC coatings. *Diam. Relat. Mater.* **2016**, *61*, 109–114. [[CrossRef](#)]
31. Fróis, A.; Aleixo, A.S.; Evaristo, M.; Santos, A.C.; Louro, C.S. Can a-C:H-sputtered coatings be extended to orthodontics? *Coatings* **2021**, *11*, 832. [[CrossRef](#)]
32. ISO 10271:2001-Dental Metallic Materials-Corrosion Test Methods; ISO (International Organization for Standardization): Geneva, Switzerland, 2001.
33. Frois, A.; Cunha, L.; Louro, C.S. Functionalization of Orthodontic Alloys with DLC Coatings. In *Proceedings of the 2019 IEEE 6th Portuguese Meeting on Bioengineering (ENBENG)*; IEEE: Lisbon, Portugal, 2019; pp. 1–4. [[CrossRef](#)]
34. Madamba, D. The Effect of Surface Treatment on Nickel Leaching from Nitinol. Master's Theses, ProQuest Dissertations Publishing, Ann Arbor, MI, USA, 2013. [[CrossRef](#)]
35. Schwan, J.; Ulrich, S.; Batori, V.; Ehrhardt, H.; Silva, S.R.P. Raman spectroscopy on amorphous carbon films. *J. Appl. Phys.* **1996**, *80*, 440–447. [[CrossRef](#)]
36. Stan, G.E.; Marcov, D.A.; Popa, A.C.; Husanu, M.A. Polymer-like and diamond-like carbon coatings prepared by RF-PECVD for biomedical applications. *Dig. J. Nanomater. Biostructures* **2010**, *5*, 705–718.
37. Ryaguzov, A.P.; Yermekov, G.A.; Nurmamyrov, T.E.; Nemkayeva, R.R.; Guseinov, N.R.; Aliaskarov, R.K. Visible Raman spectroscopy of carbon films synthesized by ion-plasma sputtering of graphite. *J. Mater. Res.* **2016**, *31*, 127–136. [[CrossRef](#)]
38. Singha, A.; Ghosh, A.; Roy, A.; Ray, N.R. Quantitative analysis of hydrogenated diamondlike carbon films by visible Raman spectroscopy. *J. Appl. Phys.* **2006**, *100*, 044910. [[CrossRef](#)]
39. Kuhta, M.; Pavlin, D.; Slaj, M.; Varga, S.; Lapter-Varga, M.; Slaj, M. Type of archwire and level of acidity: Effects on the release of metal ions from orthodontic appliances. *Angle Orthod.* **2009**, *79*, 102–110. [[CrossRef](#)] [[PubMed](#)]
40. Barrett, R.D.; Bishara, S.E.; Quinn, J.K. Biodegradation of orthodontic appliances. Part I. Biodegradation of nickel and chromium in vitro. *Am. J. Orthod. Dentofac. Orthop.* **1993**, *103*, 8–14. [[CrossRef](#)]
41. Wendl, B.; Wiltsche, H.; Lankmayr, E.; Winsauer, H.; Walter, A.; Muchitsch, A.; Jakse, N.; Wendl, M.; Wendl, T. Metal release profiles of orthodontic bands, brackets, and wires: An in vitro study. *J. Orofac. Orthop. Fortschr. Der Kieferorthopädie* **2017**, *78*, 494–503. [[CrossRef](#)] [[PubMed](#)]
42. Pound, B.G. Passive films on metallic biomaterials under simulated physiological conditions. *J. Biomed. Mater. Res. Part A* **2014**, *102*, 1595–1604. [[CrossRef](#)] [[PubMed](#)]
43. Hedberg, Y.S.; Odnevall Wallinder, I. Metal release from stainless steel in biological environments: A review. *Biointerphases* **2016**, *11*, 018901. [[CrossRef](#)]
44. Mikulewicz, M.; Chojnacka, K. Release of metal ions from orthodontic appliances by in vitro studies: A systematic literature review. *Biol. Trace Elem. Res.* **2011**, *139*, 241–256. [[CrossRef](#)]
45. Sfondrini, M.F.; Cacciafesta, V.; Maffia, E.; Scribante, A.; Alberti, G.; Biesuz, R.; Klersy, C. Nickel release from new conventional stainless steel, recycled, and nickel-free orthodontic brackets: An in vitro study. *Am. J. Orthod. Dentofac. Orthop.* **2010**, *137*, 809–815. [[CrossRef](#)]
46. Sfondrini, M.F.; Cacciafesta, V.; Maffia, E.; Massironi, S.; Scribante, A.; Alberti, G.; Biesuz, R.; Klersy, C. Chromium release from new stainless steel, recycled and nickel-free orthodontic brackets. *Angle Orthod.* **2009**, *79*, 361–367. [[CrossRef](#)] [[PubMed](#)]
47. Castro, S.M.; Ponces, M.J.; Lopes, J.D.; Vasconcelos, M.; Pollmann, M.C.F. Orthodontic wires and its corrosion—The specific case of stainless steel and beta-titanium. *J. Dent. Sci.* **2015**, *10*, 1–7. [[CrossRef](#)]
48. Castro, S.; Ponces, M.J.; Lopes, J.D.; Vasconcelos, M.; Reis Campos, J.C.; Pollmann, C. Orthodontic stainless steel wire and nickel release. In *Proceedings of the Biodental Engineering V-Proceedings of the 5th International Conference on Biodental Engineering*, Porto, Portugal, 22–23 June 2018; pp. 113–114.
49. Kao, C.-T.; Huang, T.-H. Variations in surface characteristics and corrosion behaviour of metal brackets and wires in different electrolyte solutions. *Eur. J. Orthod.* **2010**, *32*, 555–560. [[CrossRef](#)] [[PubMed](#)]
50. Pattabiraman, V.; Pai, S.; Kumari, S.; Nelivigi, N.; Sood, R.; Kumar, S. Welding of attachments in orthodontics: Technique recommendations based on a literature search. *J. Indian Orthod. Soc.* **2014**, *48*, 42–46. [[CrossRef](#)]
51. Jacoby, L.S.; Junior, V.D.S.R.; Campos, M.; de Menezes, L.M. Cytotoxic outcomes of orthodontic bands with and without silver solder in different cell lineages. *Am. J. Orthod. Dentofac. Orthop.* **2017**, *151*, 957–963. [[CrossRef](#)]
52. Freitas, M.P.M.; Oshima, H.M.S.; Menezes, L.M.; Machado, D.C.; Viezzer, C. Cytotoxicity of silver solder employed in orthodontics. *Angle Orthod.* **2009**, *79*, 939–944. [[CrossRef](#)]
53. Grimsdottir, M.R.; Gjerdet, N.R.; Hensten-Pettersen, A. Composition and in vitro corrosion of orthodontic appliances. *Am. J. Orthod. Dentofac. Orthop.* **1992**, *101*, 525–532. [[CrossRef](#)]
54. Berge, M.; Gjerdet, N.R.; Erichsen, E.S. Corrosion of silver soldered orthodontic wires. *Acta Odontol. Scand.* **1982**, *40*, 75–79. [[CrossRef](#)] [[PubMed](#)]
55. Cempel, M.; Nikel, G. Nickel: A review of its sources and environmental toxicology. *Pol. J. Environ. Stud.* **2006**, *15*, 375–382.
56. WHO (World Health Organization). *Guidelines for Drinking-Water Quality*, 4th ed.; World Health Organization: Geneva, Switzerland, 2011.

57. De Souza, R.M.; De Menezes, L.M. Nickel, chromium and iron levels in the saliva of patients with simulated fixed orthodontic appliances. *Angle Orthod.* **2008**, *78*, 345–350. [[CrossRef](#)]
58. Mikulewicz, M.; Chojnacka, K.; Woźniak, B.; Downarowicz, P. Release of metal ions from orthodontic appliances: An in vitro study. *Biol. Trace Elem. Res.* **2012**, *146*, 272–280. [[CrossRef](#)] [[PubMed](#)]
59. Staffolani, N.; Damiani, F.; Lilli, C.; Guerra, M.; Staffolani, N.J.; Beicastro, S.; Locci, P. Ion release from orthodontic appliances. *J. Dent.* **1999**, *27*, 449–454. [[CrossRef](#)]
60. Hwang, C.J.; Shin, J.S.; Cha, J.Y. Metal release from simulated fixed orthodontic appliances. *Am. J. Orthod. Dentofac. Orthop.* **2001**, *120*, 383–391. [[CrossRef](#)]
61. Hussain, H.D.; Ajith, S.D.; Goel, P. Nickel release from stainless steel and nickel titanium archwires—An in vitro study. *J. Oral Biol. Craniofacial Res.* **2016**, *6*, 213–218. [[CrossRef](#)]
62. Haddad, A.C.S.S.; Tortamano, A.; de Souza, A.L.; de Oliveira, P.V. An in vitro comparison of nickel and chromium release from brackets. *Braz. Oral Res.* **2009**, *23*, 399–406. [[CrossRef](#)]
63. Velasco-Ibáñez, R.; Lara-Carrillo, E.; Morales-Luckie, R.A.; Romero-Guzmán, E.T.; Toral-Rizo, V.H.; Ramírez-Cardona, M.; García-Hernández, V.; Medina-Solís, C.E. Evaluation of the release of nickel and titanium under orthodontic treatment. *Sci. Rep.* **2020**, *10*, 22280. [[CrossRef](#)] [[PubMed](#)]
64. Hatem, A.; Lin, J.; Wei, R.; Torres, R.D.; Laurindo, C.; Soares, P. Tribocorrosion behavior of DLC-coated Ti-6Al-4V alloy deposited by PIID and PEMS + PIID techniques for biomedical applications. *Surf. Coat. Technol.* **2017**, *332*, 223–232. [[CrossRef](#)]
65. Lin, J.; Zhang, X.; Lee, P.; Wei, R. Thick diamond like carbon coatings deposited by deep oscillation magnetron sputtering. *Surf. Coat. Technol.* **2017**, *315*, 294–302. [[CrossRef](#)]
66. Keunecke, M.; Weigel, K.; Bewilogua, K.; Cremer, R.; Fuss, H.-G. Preparation and comparison of a-C:H coatings using reactive sputter techniques. *Thin Solid Film.* **2009**, *518*, 1465–1469. [[CrossRef](#)]
67. Chowdhury, S.; Laugier, M.T.; Rahman, I.Z. Characterization of DLC coatings deposited by rf magnetron sputtering. *J. Mater. Process. Technol.* **2004**, *153–154*, 804–810. [[CrossRef](#)]
68. Louro, C.; Moura, C.W.; Carvalho, N.; Stueber, M.; Cavaleiro, A. Thermal stability in oxidative and protective environments of a-C:H cap layer on a functional gradient coating. *Diam. Relat. Mater.* **2011**, *20*, 57–63. [[CrossRef](#)]
69. Ferrari, A.C.; Robertson, J. Interpretation of Raman spectra of disordered and amorphous carbon. *Phys. Rev. B* **2000**, *61*, 14095–14107. [[CrossRef](#)]
70. Zhang, L.; Wei, X.; Lin, Y.; Wang, F. A ternary phase diagram for amorphous carbon. *Carbon* **2015**, *94*, 202–213. [[CrossRef](#)]
71. Buijnsters, J.G.; Gago, R.; Jiménez, I.; Camero, M.; Agulló-Rueda, F.; Gómez-Aleixandre, C. Hydrogen quantification in hydrogenated amorphous carbon films by infrared, Raman, and x-ray absorption near edge spectroscopies. *J. Appl. Phys.* **2009**, *105*, 093510. [[CrossRef](#)]
72. Malik, A.U.; Mayan Kutty, P.C.; Siddiqi, N.A.; Andijani, I.N.; Ahmed, S. The influence of pH and chloride concentration on the corrosion behaviour of AISI 316L steel in aqueous solutions. *Corros. Sci.* **1992**, *33*, 1809–1827. [[CrossRef](#)]
73. Akpanyung, K.; Loto, R. Pitting corrosion evaluation: A review. *J. Phys. Conf. Ser.* **2019**, *1378*, 022088. [[CrossRef](#)]
74. Chen, J.S.; Lau, S.P.; Sun, Z.; Chen, G.Y.; Li, Y.J.; Tay, B.K.; Chai, J.W. Metal-containing amorphous carbon films for hydrophobic application. *Thin Solid Film.* **2001**, *398–399*, 110–115. [[CrossRef](#)]
75. Sun, L.; Guo, P.; Li, X.; Wang, A. Comparative study on structure and wetting properties of diamond-like carbon films by W and Cu doping. *Diam. Relat. Mater.* **2017**, *73*, 278–284. [[CrossRef](#)]
76. Gotzmann, G.; Beckmann, J.; Wetzels, C.; Scholz, B.; Herrmann, U.; Neunzehn, J. Electron-beam modification of DLC coatings for biomedical applications. *Surf. Coat. Technol.* **2017**, *311*, 248–256. [[CrossRef](#)]
77. Ishige, H.; Akaike, S.; Hayakawa, T.; Hiratsuka, M.; Nakamura, Y. Evaluation of protein adsorption to diamond-like carbon (DLC) and fluorinedoped DLC films using the quartz crystal microbalance method. *Dent. Mater. J.* **2019**, *38*, 424–429. [[CrossRef](#)] [[PubMed](#)]
78. Ilic, E.; Pardo, A.; Suter, T.; Mischler, S.; Schmutz, P.; Hauert, R. A methodology for characterizing the electrochemical stability of DLC coated interlayers and interfaces. *Surf. Coat. Technol.* **2019**, *375*, 402–413. [[CrossRef](#)]
79. Kobayashi, S.; Ohgoe, Y.; Ozeki, K.; Hirakuri, K.; Aoki, H. Dissolution effect and cytotoxicity of diamond-like carbon coatings on orthodontic archwires. *J. Mater. Sci. Mater. Med.* **2007**, *18*, 2263–2268. [[CrossRef](#)]
80. Ohgoe, Y.; Kobayashi, S.; Ozeki, K.; Aoki, H.; Nakamori, H.; Hirakuri, K.K.; Miyashita, O. Reduction effect of nickel ion release on a diamond-like carbon film coated onto an orthodontic archwire. *Thin Solid Film.* **2006**, *497*, 218–222. [[CrossRef](#)]
81. Porcayo-Calderon, J.; Casales-Diaz, M.; Salinas-Bravo, V.M.; Martinez-Gomez, L. Corrosion performance of Fe-Cr-Ni Alloys in artificial saliva and mouthwash solution. *Bioinorg. Chem. Appl.* **2015**, *2015*. [[CrossRef](#)] [[PubMed](#)]